RSC Applied Interfaces

Accepted Manuscript

This article can be cited before page numbers have been issued, to do this please use: R. Nandi, M. U. Saeed and C. Chen, *RSC Appl. Interfaces*, 2026, DOI: 10.1039/D6LF00103C.

ROYAL SOCIETY OF CHEMISTRY

rsc.li/RSCApplInter

View Article Online
DOI: 10.1039/D6LF00103C

Decoding Interfacial Phenomena in Liquid Crystal Sensors: Mechanisms, Metrology, and Performance

Rajib Nandi, Muhammad Umer Saeed and Chih-Hsin Chen*

Department of Chemistry, Tamkang University, New Taipei City 25137, Taiwan

*To whom correspondence should be addressed.

Email: chc@mail.tku.edu.tw

View Article Online
DOI: 10.1039/D6LF00103C

Abstract

Over the past two decades, liquid crystal (LC)–based sensors have emerged as powerful, versatile soft-matter platforms for transducing molecular recognition events into macroscopic optical signals. This capability arises from the intrinsic long-range orientational order and exceptional sensitivity to interfacial anchoring energies. Although advances in new LC materials and surface functionalization strategies have greatly enhanced the sensitivity and selectivity of LC-based sensing devices, the interfacial phenomena that govern alignment and signal transduction remain insufficiently understood. This Perspective critically decodes how interfacial structure, chemistry, and dynamics collectively dictate LC sensing behavior. We summarize the fundamental mechanisms underlying LC-interfacial interactions, assess current metrological approaches for probing these dynamic boundaries, and establish correlations between interfacial properties and key sensing metrics such as sensitivity, selectivity, and stability. By integrating insights from interfacial science with performance evaluation, we identify emerging opportunities for precision interfacial engineering through advanced characterization, multiscale modeling, and data-driven analysis, thereby providing a rational framework for designing next-generation LC-based sensors.

Keywords: Liquid crystal-based sensors; Interfacial phenomena; Surface alignment and anchoring; Metrology and characterization; Rational interfacial engineering.

View Article Online
DOI: 10.1039/D6LF00103C

1. Introduction

Owing to their long-range orientational order, self-assembly capability, and extraordinary sensitivity to interfacial interactions, liquid crystals (LCs) can amplify subtle molecular events at interfaces into macroscopic optical responses, making LC–based sensors powerful soft-matter transduction platforms.[1,2] Over the past decade, research efforts have largely focused on tailoring LC materials, designing functional alignment layers, and improving sensing sensitivity and selectivity through chemical surface modification.[3,4] These strategies have significantly broadened the scope of LC-based sensing technologies, enabling the detection of diverse chemical and biological targets in environmental monitoring, biomedical diagnostics, and food safety.[3-13] While these advances have significantly expanded the scope and performance of LC sensors, the underlying interfacial phenomena that dictate LC alignment and signal transduction remain insufficiently understood and lack a unified mechanistic framework.

The interface between the LC phase and its contacting medium—whether solid, liquid, or gaseous—acts as the dynamic stage where molecular recognition, adsorption, and orientation transitions occur. Small perturbations in interfacial chemistry, molecular packing, or surface energy can alter the anchoring conditions of LC molecules. These interfacial processes ultimately govern the sensitivity, selectivity, and stability of LC sensors. Decoding these interfacial phenomena and establishing how molecular events at the boundary are amplified into measurable optical signals, represents the key to transforming LC sensors from empirically optimized systems into rationally designed analytical devices. In this Perspective, we organize current knowledge of LC sensors through an interfacial framework that integrates three interconnected dimensions: (i) mechanisms, describing the molecular processes governing LC alignment and interfacial coupling; (ii) metrology, encompassing experimental and analytical approaches for probing interfacial structure and dynamics; and (iii) performance, linking

View Article Online
DOI: 10.1039/D6LF00103C

interfacial properties to key sensing metrics such as sensitivity, selectivity, and stability. To provide an overview of this concept, Fig. 1 schematically illustrates how interfacial phenomena bridge molecular interactions and macroscopic sensing behavior in LC systems. By integrating insights from interfacial science, soft-matter physics, and analytical sensing, we highlight emerging opportunities for rationally engineering LC interfaces to achieve improved sensor performance.

Although a variety of optical sensing platforms, including photonic crystal and photonic crystal fiber (PCF)-based sensors, have demonstrated remarkable performance in biomedical diagnostics, environmental monitoring, and AI-assisted sensing applications, their signal transduction mechanisms are fundamentally different from those of LC-based sensors. Whereas photonic sensors primarily rely on refractive index modulation and optical resonance effects, LC-based sensors operate through analyte-induced changes in interfacial anchoring and orientational order. Therefore, this Perspective focuses specifically on the interfacial phenomena that govern LC sensing behavior and determine sensing performance.

View Article Online
DOI: 10.1039/D6LF00103C

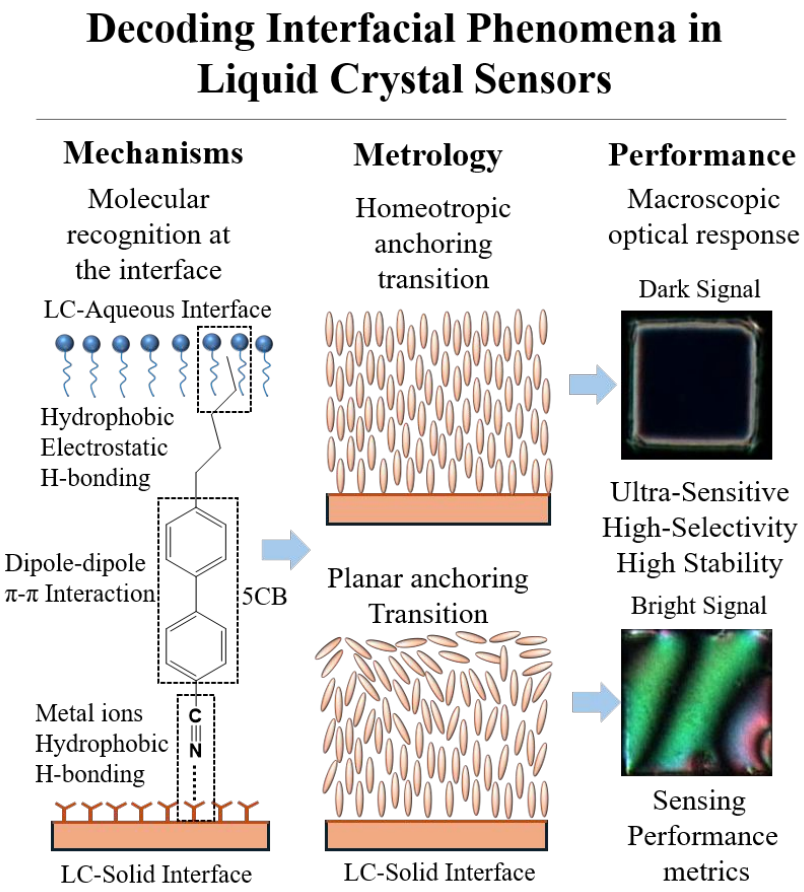

Fig 1. Conceptual illustration of interfacial phenomena governing LC sensor behavior. The schematic highlights the progression from molecular interactions at the functionalized interface (Mechanisms, left), through LC alignment transitions driven by interfacial energy minimization and molecular adsorption (Metrology, center), to the resulting optical signal output that defines sensing performance (Performance, right). Interfacial events such as complexation, imbalance in amphiphilicity, hydrogen bonding, and charge transfer trigger reorientation of LC molecules, which is optically amplified into macroscopic responses. This *mechanisms–metrology–performance* framework underscores how understanding and controlling interfacial processes enable rational design of next-generation LC-based sensors.

2. Mechanisms: interfacial phenomena as the foundation of liquid crystal sensing

2.1 Interfaces Control LC Orientation

Liquid crystal (LC)-based sensors can be broadly classified into lyotropic and thermotropic systems. Lyotropic LCs are formed through the self-assembly of amphiphilic molecules in a solvent and have attracted considerable attention for biosensing applications due to their biocompatibility, structural diversity, and tunable interfacial properties.[14,15] In contrast,

View Article Online
DOI: 10.1039/D6LF00103C

thermotropic LCs undergo phase transitions primarily in response to temperature and are widely employed in optical sensing because of their well-defined birefringence, elastic properties, and anchoring behavior.[3–5] Among thermotropic LCs, calamitic nematic phases are the most extensively studied and have been widely utilized for the detection of gases, chemical analytes, and biomolecules in aqueous environments. Another important class is cholesteric liquid crystals (CLCs), which possess a self-organized helical structure that selectively reflects light at wavelengths determined by the helical pitch. External stimuli, including chemicals, biomolecules, temperature, humidity, mechanical stress, and electric fields, can modify the pitch, refractive index, or molecular organization of the cholesteric phase, leading to measurable color changes or shifts in the reflected wavelength.[16,17] In this Perspective, we focus primarily on interface-sensitive thermotropic LCs, particularly nematic systems, because their orientational order is highly responsive to interfacial perturbations, making them effective transducers for molecular recognition and sensing events. Whether an LC is in contact with a solid substrate, an aqueous phase, or a gas, the interface serves as a molecular and energetic control center that determines the director field and, thus, the optical output of the sensing platform. Consequently, the sensing signal arises not from bulk LC properties alone, but from the balance between interfacial free energy minimization and specific molecular interactions occurring at the LC interface. Unlike liquid crystal display (LCD) where LCs are symmetrically confined between two solid alignment layers to enforce uniform anchoring, LC-based sensors deliberately incorporate at least one open or fluid interface to enable analyte access as shown in Fig. 2. Depending on the sensing format, LCs may be organized in sandwich cells, supported thin films, TEM-grid cavities, or dispersed microdroplets,[5,6] yet all configurations can be traced to three dominant interfacial regimes:

- LC/solid interfaces – anchoring strength, surface chemistry, and nanoscale topography define baseline director orientation and defect landscape.

View Article Online
DOI: 10.1039/D6LF00103C

- LC/air interfaces – volatile analytes adsorb or diffuse through the LC–air interface, modifying interfacial energy and triggering realignment.
- LC/aqueous interfaces – ions, amphiphiles, and biomolecules partition or adsorb at the LC–water interface, reorganizing interfacial structure and inducing orientational transitions.

At LC/solid interfaces, the alignment layer establishes baseline director orientation of LC through a combination of surface chemistry, molecular ordering, and nanoscale topography. Classical alignment materials such as rubbed polyimide promote planar anchoring, whereas silane-based modifiers such as DMOAP induce strong homeotropic alignment through long-chain hydrophobic packing and electrostatic interactions.[3] Functionalized or surfactant-treated substrates further tune anchoring energy—planar, tilted, or perpendicular—via van der Waals forces, hydrogen bonding, or dipolar coupling. In LC-based sensors, this predefined anchoring state becomes an interfacial "reference point" that is perturbed when analytes adsorb, displace surface ligands, or reorganize the interfacial energy landscape, resulting in a measurable reorientation event.[1,3,5-7]

At LC/air interfaces, the LC phase is exposed to volatile analytes whose adsorption, diffusion, or reactive interaction alters surface polarity and interfacial free energy. Organic vapors, gaseous oxidants, or coordination-active species can diffuse inward from the LC-air boundary and induce localized reordering that propagates toward the LC/solid interface beneath (Figs. 2 and 3A). This top-down perturbation pathway enables highly sensitive vapor sensing without the need for covalent surface functionalization, as even minor shifts in interfacial tension or molecular packing are optically amplified by the LC phase.[6,8,12]

At LC/aqueous interfaces, particularly LC–water boundaries, orientational order is governed by interfacial tension and the intrinsic immiscibility between LCs and water. Nematic phases such as 5CB or E7 typically adopt planar alignment at the aqueous interface but are exquisitely sensitive to amphiphiles, ions, and biomolecules that adsorb or partition into the

View Article Online
DOI: 10.1039/D6LF00103C

boundary region.[1] Surfactants, metal ions, or proteins can reorganize the interfacial layer and trigger abrupt transitions between bright and dark optical states under crossed polarizers, which is an effect that forms the basis of many label-free biochemical LC assays (Figs. 2 and 3B).[3,5,13] Lipid- and surfactant-functionalized interfaces represent key examples of interfacial self-assembly in LC sensing platforms.[18,19] Amphiphilic molecules can spontaneously organize at LC–aqueous interfaces to form ordered interfacial layers, whose molecular packing, orientation, and surface coverage regulate LC anchoring conditions. Target analytes may disrupt, reorganize, or competitively interact with these amphiphilic layers, thereby altering interfacial free energy and triggering LC realignment. The amplification of such molecular-scale interfacial changes into macroscopic optical responses forms the basis of many LC-based biosensing, chemical sensing, and environmental monitoring applications.

The sensing performance of LC platforms is governed by the coupled effects of interfacial structure, chemistry, and dynamics. Interfacial structure determines the spatial arrangement of binding sites, surface morphology, and molecular organization, which together define the anchoring environment experienced by LC molecules. Interfacial chemistry controls the specific interactions between mesogens and the sensing layer, including hydrogen bonding, electrostatic interactions, van der Waals forces, coordination interactions, and redox-driven transformations. These interactions alter surface free energy and anchoring strength, ultimately triggering LC reorientation. Simultaneously, interfacial dynamics, including analyte adsorption–desorption processes, diffusion, reaction kinetics, and relaxation of surface-bound species, govern the temporal evolution, sensitivity, and reversibility of the sensing response. These three factors are intrinsically coupled through the anchoring energy landscape, which serves as the thermodynamic bridge connecting molecular-scale interfacial events to LC director reorientation and macroscopic optical outputs.

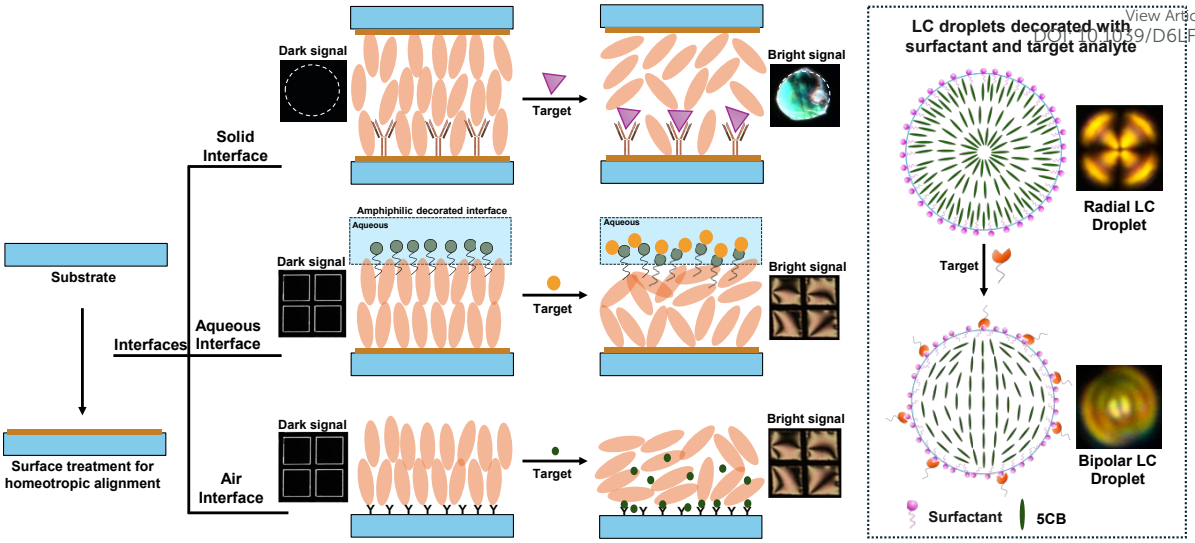

Fig. 2. Liquid crystal sensing mechanisms across different interfaces. The schematic illustrates LC alignment and corresponding optical responses at solid, aqueous, and air interfaces. Surface treatment promotes initial homeotropic alignment, producing a dark optical signal. Introduction of target analytes disrupts homeotropic alignment, inducing a transition to planar alignment and generating a bright signal. On the right, LC droplets dispersed in aqueous solution and decorated with surfactants initially exhibit radial alignment. Upon exposure to target analytes, the configuration transitions to bipolar alignment, forming the basis for LC-based biosensing platforms.

2.2 Interfacial Interactions Governing Alignment Transitions in LC

The alignment state of LCs at an interface is not determined by a single dominant interaction, but by the dynamic superposition of multiple intermolecular interactions. Nematic LCs such as 5CB and E7 possess a polar cyano group, rigid aromatic cores, and hydrophobic alkyl chains, enabling simultaneous engagement in hydrophobic interactions, hydrogen bonding, π–π stacking, dipole–dipole coupling interactions and electrostatic effects. These forces collectively define the interfacial free-energy landscape that stabilizes the initial LC orientation. Crucially, they also represent the molecular "levers" through which analytes reprogram that orientation.

• Hydrophobic interactions

Hydrophobic interaction between nonpolar alkyl chains (of amphiphiles) within LCs minimize interfacial free energy at hydrophobic solid or LC–aqueous boundaries, thereby favoring

View Article Online
DOI: 10.1039/D6LF00103C

homeotropic alignment. Upon introduction of target analytes, amphiphiles or surfactants disrupts this balance and often induces a transition to planar alignment, forming the basis of many LC–water biosensing platforms.[7]

• Hydrogen bonding

The nitrile group in 5CB and related nematic LCs acts as a hydrogen-bond acceptor, enabling specific H-bonding interactions with –OH, –COOH, or $–NH_2$ functionalities on substrates or analytes. Depending on the geometry and density of bonding sites, this interaction can either reinforce homeotropic anchoring or induce a well-defined planar state.[8,9]

• π–π stacking interactions

Aromatic LCs engage in π–π stacking with conjugated probe molecules, adsorbed polycyclic compounds, or π-rich surface coatings. This interaction has been exploited to create LC sensors that selectively reorient in the presence of aromatic pollutants, phenolic toxins, or dye molecules.[10,11,20]

• Dipole–dipole interactions and electrostatic effects

At polar or charged interfaces, long-range dipolar coupling can dominate anchoring behavior. For example, ion adsorption at elevated pH can generate an electric double layer that biases nematic LCs toward homeotropic alignment, while cation exchange or charge inversion can trigger the opposite transition.[5,21]

The sensing event, therefore, does not arise from the formation or disruption of a single interaction but from the competitive rebalancing of multiple interfacial forces. This makes LC interfaces inherently programmable. That is, even subtle analyte-induced perturbations can reorganize the energy hierarchy of these forces, producing sharp and optically amplified alignment transitions.

View Article Online
DOI: 10.1039/D6LF00103C

Beyond these specific intermolecular interactions, LC alignment is fundamentally governed by the competition between surface anchoring forces and interfacial free-energy minimization. Surface morphology, chemical heterogeneity, and the spatial distribution of functional groups determine the local anchoring strength and the threshold energy required for LC reorientation. Molecular-level perturbations introduced by analyte binding are subsequently amplified through long-range elastic coupling within the LC bulk, enabling highly sensitive optical detection and directly influencing sensing metrics such as sensitivity, response time, selectivity, and reversibility.

2.3 Transduction of Interfacial Events into Optical Signal

The sensing capability of LCs arises from their unique combination of anisotropic optical properties and long-range orientational order. Nematic LCs, characterized by the orientational order of the director (*n*), possess anisotropic optical properties (birefringence) and elasticity, which allow energy storage via splay, bend, and twist deformations. The elastic energy per unit area stored in a strained LC film can be approximated as K/h, where K is the elastic constant and h the film thickness; for a typical LC such as 5CB, this energy ($\sim 10^{-5}$ J m^{-2}) is comparable to the surface anchoring energy (W) (10^{-6} – 10^{-5} J m^{-2}), highlighting the sensitivity of LC orientation to small interfacial perturbations.[22] When analyte molecules interact with functionalized LC interfaces through ligand binding, chemical reactions, adsorption or complexation, they perturb the delicate balance between elastic and anchoring energies. Consequently, due to the intrinsic long range of orientational order in LC, analyte molecules change the alignment of LC. Therefore, these molecular-level interactions alter short- and long-range interfacial forces, reorganizing the director field and generating elastic strain that manifests as changes in birefringence, optical textures, or electro-optical responses. As a result, LC-based systems act as optical amplifiers, converting nanoscale interfacial chemistry into

View Article Online
DOI: 10.1039/D6LF00103C

measurable macroscopic signals. This capability enables label-free, real-time detection of chemical and biological stimuli.

2.4 Elastic–Anchoring Balance in Thin LC Films

The magnitude of optical response is governed by the competition between bulk elasticity and surface anchoring. This interplay determines whether the LC behaves as a surface-dominated or elasticity-dominated system and thus controls the amplification of interfacial perturbations. A key descriptor of this balance is the ratio $(K/h)/W$, where K is the elastic constant, h the film thickness, and W the anchoring strength. The corresponding extrapolation length, $\xi = K/W$, defines the characteristic distance over which the interface can impose orientational order. For typical nematic LCs ($K \approx 10^{-12}$ N, $W \approx 10^{-6}$ J m^{-2}), ξ is on the order of ~1 μm.[23] When $h \ll \xi$, elasticity dominates, suppressing anchoring-induced transitions and producing metastable or frustrated director states with reduced birefringence contrast. Such behavior is frequently observed in ultrathin LC films (10–100 nm) or in systems where W is weakened through short-chain silanes, dilute SAMs, or physisorbed surfactants.[24-27-21] Conversely, when $W \gg K/h$, anchoring dominates and the LC director closely follows interfacial perturbations. Strengthening anchoring—via long-chain SAMs, covalent surface attachment, or nanotextured substrates—restores surface control and enhances the magnitude and stability of optical transitions.[10,26] Maximum sensing sensitivity is typically achieved near the condition $K/h \approx W$, in which elastic and anchoring energies are comparable and even subtle analyte adsorption events can tip the balance, yielding large and rapid optical responses. When the elastic and anchoring energies are tuned into this responsive regime, LCs behave not merely as passive transducers, but as self-reporting soft materials that autonomously convert interfacial chemistry into optical feedback, setting the stage for the self-regulating behaviors introduced in the following section.

View Article Online
DOI: 10.1039/D6LF00103C

2.5 Self-reporting and Self-Regulating Liquid Crystals

Beyond signal transduction, LCs possess an intrinsic capacity for self-reporting and self-regulation because their orientational order couples interfacial events to long-range elastic fields as shown in Fig. 3C.[13] When immiscible inclusions (solid particles, droplets, gas bubbles, or molecular assemblies) are dispersed within a nematic LC, the balance between bulk elastic energy (~KR) and interfacial anchoring energy (~WR²) determines whether the LC director field remains defect-free or forms topological distortions.[23,27] For typical thermotropic LCs such as 5CB ($K \approx 10^{-12}$ N, $W \approx 10^{-6}$ J m^{-2}), the characteristic crossover length $K/W \approx 1$ μm, meaning inclusions larger than this threshold generate defect structures with elastic energies of 10^3–10^4 kBT—sufficient to mediate long-range repulsion, assemble ordered lattices, and prevent coalescence.[28,29] These coupled elastic–anchoring fields allow nematic LCs to report molecular-scale perturbations through changes in birefringence, defect topology, or optical texture, without external labels or amplification schemes.[25] At the same time, the same elastic feedback enables self-regulation: LC droplets can restructure, reorient, or annihilate defects to minimize free energy, producing autonomous responses to thermal, chemical, or mechanical triggers.[13,28,29] Functionalization of either the LC phase or the dispersed phase further extends this behavior toward programmable actuation, controlled release platforms, and adaptive sensing materials.[13] Together, these properties position LCs not only as passive transducers but as active soft matter, capable of integrating sensing, reporting, and regulation into a single material framework, bridging molecular recognition with mesoscopic mechanics.

Taken together, the mechanisms discussed in this section establish a central principle: LC–based sensing is not driven by the intrinsic responsiveness of the LC phase, but by the optical amplification of interfacial molecular events. The LC does not only report the analyte itself, but it reports the reorganization of anchoring energy, defect topology, and elastic fields initiated at the interface. In this sense, LCs function not as conventional “stimuli-responsive

View Article Online
DOI: 10.1039/D6LF00103C

materials," but as interfacial amplifiers capable of converting nanometer-scale chemistry into millimeter-scale optical contrast. Recognizing this shift—from "the LC responds" to "the LC reveals the interface"—is essential for transitioning the field from empirical optimization to rational, interface-engineered sensing design. This conceptual turning point provides the foundation for the performance correlations and metrological challenges addressed in Section 3.

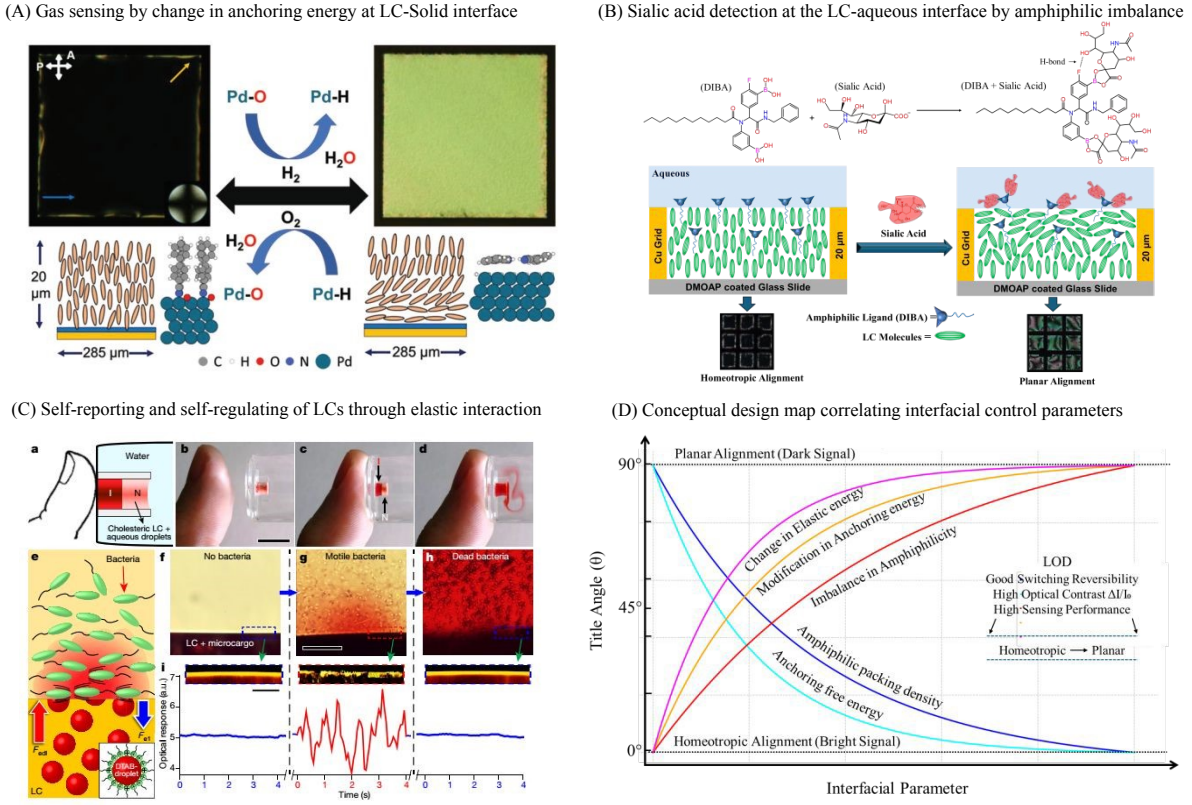

Fig. 3. (A) Schematic illustrations and polarized optical micrographs showing LC orientation changes upon sequential exposure to H_2 (1 atm, 30 s) followed by O_2 (1 atm) in 20 μm thick films of nematic 5CB supported on Pd (8 ± 0.5 ML)/Au films (Reproduced with permission from ref 11). (B) Schematic illustration of the sensing mechanism for sialic acid detection using a boronic acid–based amphiphile (DIBA) doped LC. DIBA acts as both an amphiphilic alignment agent and sensing probe. Interaction of its boronic acid groups with sialic acid at the LC/aqueous interface alters the amphiphilic balance of DIBA, triggering an optical transition in the LC from a dark to bright state. (Reproduced with permission from ref 12). (C) Self-regulated release of microcargo from LCs triggered either by the heat of a human finger or by motile bacteria that generate interfacial shear stresses. (Reproduced with permission from ref 13). (D) Conceptual design map correlating interfacial control parameters with LC alignment states and sensing performance. The x-axis represents interfacial parameters (e.g., amphiphile packing density, anchoring free energy, elastic energy, and deviation in amphiphilicity), while the y-axis shows the LC director tilt angle (θ), ranging from homeotropic (0°) to planar (90°).

View Article Online
DOI: 10.1039/D6LF00103C

Colored curves illustrate how different interfacial factors drive alignment transitions, from which sensing performance metrics such as the LOD emerge.

3. Metrology: characterizing and visualizing interfacial processes

3.1 Why Interfacial Metrology Matters in LC-Based Sensing

The previous section established that LCs do not function as intrinsically "stimuli-responsive" materials, but as optical amplifiers of interfacial molecular events. This reframing shifts the core scientific challenge of LC-based sensing. That is, if the sensing signal originates from the chemistry and mechanics of the LC/solid, LC/aqueous, and LC/gas interfaces, then the primary limitation of the field is no longer how strongly the LC responds, but how precisely we can observe, quantify, and correlate what happens at the interface. However, the molecular interactions that trigger LC reorientation, such as hydrogen bonding, ligand exchange, ion pairing, amphiphile assembly, or defect nucleation, occur on nanometer length scales and millisecond-to-second timescales, far below the resolution of the techniques most commonly used in LC research. Unlike rigid solid–solid boundaries, LC interfaces are soft, reconfigurable, partially buried, and continuously evolving, meaning that their structure cannot be captured by static or ex situ characterization.

Three fundamental constraints make LC interfaces exceptionally difficult to interrogate:

1. Multiscale coupling: molecular (Å to nm) → interfacial (nm to μm) → elastic/optical (μm to mm).
2. Buried-interface problem: the sensing event occurs beneath the LC phase, not on an exposed surface.
3. Operando limitation: most surface-analytical tools cannot probe the soft-interface during sensing, only before or after.

As a consequence, interfacial processes in LC-based sensors are still inferred indirectly from optical textures, rather than measured at the place where sensing actually begins.

View Article Online
DOI: 10.1039/D6LF00103C

To clarify the current methodological landscape, Table 1 summarizes the most widely used techniques, the type of interfacial information they provide, and their principal limitations when applied to LC interfaces. The comparison highlights a critical point: no single technique can simultaneously resolve chemistry (who binds), orientation (how LCs respond), and dynamics (when the event occurs), revealing that the frontier of LC sensing not only relies on material innovation, but also on metrology innovation. This recognition sets the stage for the following sections: if LC sensors are to transition from empirical texture-based interpretation to predictive, interface-engineered design, the next generation of tools must move toward operando, correlative, and data-driven interfacial characterization.

Table 1. Commonly used experimental techniques for probing interfacial phenomena in LC-based sensors.

Technique	Operating Principle / Measured Parameter	Information Obtained at LC Interfaces	Typical Use in LC-Based Sensing	Key Advantages	Key Limitations	Ref.
Polarized Optical Microscopy (POM)	Birefringence contrast under crossed polarizers	Director orientation, anchoring transitions, defect structures	Monitoring optical response at LC/solid, LC/air, and LC/aqueous interfaces	Real-time, label-free, simple	Qualitative; no molecular-scale detail	3, 22, 26
Fluorescence or Bright-Field Microscopy (with labeled analytes)	Spatial mapping of tagged species at interface	Localization and adsorption kinetics of biomolecules or surfactants	Tracking binding events at LC–water interfaces	High specificity; dynamic imaging	Requires labeling; probe may alter interface	30
Electro-Optical Measurements (V–T curves, switching time)	Field-induced reorientation of LC director	Anchoring strength, elastic constants, interfacial switching thresholds	Quantifying anchoring changes after analyte binding	Quantitative; sensitive to subtle W changes	Requires electrodes and controlled cell geometry	1, 26
Tilt Angle / Retardance Measurement (Berek compensator, Michel–Levy)	Optical retardation used to infer tilt angle (θ)	Estimates director tilt in partially aligned states	Detecting intermediate LC states between planar/homeotropic	Semi-quantitative; works in real time	Averages over area; poor spatial resolution	26
Zeta Potential (LC droplets only)	Electrokinetic potential at LC–water interface	Charge environment and adsorption of ionic species	Studying surfactant/ion regulation in LC emulsions	Quantifies interfacial charge	Only applicable to droplets, not thin films	4, 9

Contact Angle Goniometry	Wettability and surface energy analysis	Surface polarity changes after modification or adsorption	Evaluating functionalization of solid substrates	Simple, macroscopic	No LC present; ex situ only	22, 26

View Article Online
DOI: 10.1039/D6LF00103C

3.2 Beyond Bright and Dark in LC States: Quantifying Intermediate Orientational States

Although LC-based sensing is often described in terms of two optical extrema, i.e., homeotropic (dark) and planar (bright), most real sensing events do not proceed through an instantaneous binary switch. Instead, the LC passes through intermediate, partially tilted, or frustrated alignment states, where anchoring, elastic torque, and adsorption kinetics are not yet equilibrated. These intermediate orientational states play a critical scientific role, as they directly influence key performance parameters such as response time, sensitivity, and detection limit. They also serve as the missing link between interfacial molecular events and bulk LC alignment, often containing the true mechanistic signature of the sensing process. However, despite their importance, these states remain poorly resolved, largely because most optical techniques can only report changes in transmitted intensity without providing quantitative access to the underlying molecular tilt angle (θ) or azimuthal rotation (φ) with adequate spatial or temporal resolution. Current practice primarily relies on birefringence-based retardance estimation using tilting compensators, which yield only a bulk-averaged θ and gives no information on φ. As a result, different interfacial states can produce indistinguishable grayscale images, hiding crucial mechanistic details of LC alignment and sensing behavior.

A next-generation metrology strategy will require correlative measurement, where optical mapping is coupled to at least one of the following:

- Raman tensor orientation mapping (θ, φ)
- fluorescence polarization (molecular-level orientation)
- nanoscale mechanical/surface force mapping (elastic response)
- AI-assisted texture reconstruction (θ–φ field extraction from images)

View Article Online
DOI: 10.1039/D6LF00103C

Only when intermediate states are quantitatively measured, rather than merely inferred from optical textures, can LC sensing progress from qualitative observation to predictive, model-driven design.

3.3 From Observation to Prediction: Toward Operando and Data-Driven LC Metrology

The current metrology of LC-based sensing remains largely observational: interfacial events are inferred from optical textures rather than measured directly at the interface. To enable predictive, interface-engineered LC sensors, measurement strategies must evolve from ex situ, single-mode, and qualitative toward operando, multimodal, and data-driven approaches.

(1) Operando Interfacial Probing

Most surface-analytical methods used in LC research, such as X-ray photoelectron spectroscopy (XPS), Raman spectroscopy, atomic force microscopy (AFM), and infrared (IR) spectroscopy, are powerful but fundamentally ex situ, and therefore unable to capture adsorption, binding, or anchoring transitions during sensing. Operando tools such as phase-modulated infrared reflection–absorption spectroscopy (IRRAS), sum-frequency generation (SFG) vibrational spectroscopy, and microfluidic-integrated Raman platforms now allow real-time monitoring of LC–water and LC–air interfaces with molecular specificity.[31,32] In addition to the techniques summarized in Table 1, several advanced interface-sensitive characterization methods can provide complementary information on LC interfacial processes. Surface plasmon resonance (SPR) enables real-time monitoring of adsorption kinetics and binding events at functionalized interfaces. X-ray reflectometry (XRR) and neutron reflectometry (NR) can probe molecular layering, interfacial density profiles, and film thickness with sub-nanometer resolution. Cryogenic transmission electron microscopy (Cryo-TEM) offers structural visualization of interfacial assemblies, while Kelvin probe force microscopy (KPFM) can map local surface potential distributions and charge heterogeneity. These techniques may provide

View Article Online
DOI: 10.1039/D5LF00103C

valuable information on adsorption kinetics, interfacial mass transport, molecular layering, viscoelastic properties, and surface potential distributions.[33,34] Nevertheless, each technique possesses inherent limitations, including ensemble averaging effects, limited temporal resolution, restricted accessibility to specialized instrumentation, or difficulties associated with probing buried and dynamically evolving LC interfaces under realistic sensing conditions.

Beyond conventional electro-optic readouts based on POM, advanced spectroscopic, chiroptical, and photonic approaches can further expand the analytical capabilities of LC-based sensing platforms. For example, circular dichroism (CD) spectroscopy provides complementary information on chiral molecular organization, guest-induced structural changes, and supramolecular chirality within LC assemblies. Recent studies on chiral LC supramolecular assemblies have further demonstrated that chirality transfer and amplification can be used to modulate optical activity and enable chiroptical signal generation.[35] In chiral and cholesteric LC systems, guest molecules or target analytes can modulate the helical pitch, molecular ordering, or chiroptical response, leading to measurable changes in selective reflection, CD signals, or colorimetric output.[36] These chiral LC-based sensing strategies provide additional opportunities for molecular recognition, stereochemical discrimination, and improved sensing specificity. In addition, emerging signal transduction strategies based on fluorescence readout of LC ordering transitions and LC-integrated holographic metasurfaces may further enrich LC sensing by offering enhanced sensitivity, multimodal optical responses, and opportunities for quantitative signal amplification.[37,38] Collectively, these approaches extend LC sensing beyond conventional birefringence-based detection and provide new avenues for multiplexed, highly selective, and information-rich analytical platforms.

(2) Correlative Multimodal Characterization

View Article Online
DOI: 10.1039/D6LF00103C

No single technique can simultaneously capture interfacial chemistry, director orientation, and elastic response. Correlated approaches, e.g., POM coupled with Raman tensor mapping, electro-optical switching paired with anchoring force measurements, or defect imaging combined with nanomechanical mapping, could provide a route to directly link interfacial structure → LC alignment → sensing output.[39] Future progress will therefore rely on correlative multimodal metrology frameworks that integrate complementary techniques to achieve a holistic understanding of interfacial phenomena across multiple length and time scales.

(3) AI-Assisted Optical and Defect Analytics

Machine-learning analysis of birefringence textures enables quantitative extraction of tilt angle, azimuthal rotation, and defect topology from standard POM images.[40] Emerging models can invert optical textures to predict analyte concentration, adsorption kinetics, or anchoring energy changes in real time.[41]

Advancing LC sensing will require metrology capable of visualizing the interface as it operates, rather than only before or after the sensing event. The next phase of progress depends on the integration of operando spectroscopy, correlative imaging, and AI-assisted analysis to directly link molecular-scale interfacial processes with macroscopic optical responses. In this context, the ability to observe the interface chemically, structurally, and dynamically is not a secondary characterization step, but the necessary foundation for transforming LC sensors from empirically tuned optical devices into predictively engineered interfacial systems. Metrology is therefore not an accessory to sensing; it is the enabling condition for controlling it.

4. Performance: bridging interface science and sensing metrics

4.1 Why LC Sensing Performance Must be Defined at the Interface Level

View Article Online
DOI: 10.1039/D6LF00103C

The performance of LC-based sensors is conventionally judged using macroscopic metrics such as LOD, response time, contrast ratio, selectivity, and reversibility. However, these output metrics are not intrinsic properties of the LC itself but arise from the interfacial chemistry that dictates its alignment. As established in Section 2, LCs do not "sense" analytes directly; they amplify interfacial molecular events into optical or electro-optical signals. Yet, in most published LC sensor reports, the interface remains a black box: surface chemistry is rarely quantified, anchoring energy is seldom measured, and alignment transitions are discussed phenomenologically rather than mechanistically. As a result, two systems with similar chemical recognition elements may demonstrate performance differences spanning orders of magnitude, not because of analytical design, but because of undocumented variations in interfacial parameters such as surface energy, defect density, or amphiphile packing.[42,43] This gap between what the LC reports (optical state) and what actually controls the response (interfacial energetics) is the central limitation preventing LC-based sensing from evolving into a predictive design framework. To enable reproducibility, rational optimization, and AI-assisted screening, sensing performance must therefore be redefined not merely as an optical output, but as a measurable function of interfacial parameters.

4.2 Establishing Interface–Alignment–Performance Correlations

A unifying design principle for LC sensors can be formulated through a three-level causal chain:

Interfacial property → LC alignment state → Sensing performance metric

In this framework, the interface determines the anchoring energy landscape, which sets the molecular tilt, defect topology, or director ordering of the LC phase, which in turn defines measurable outputs such as grayscale intensity, birefringence, or switching threshold. Importantly, each link in this chain can be quantified rather than described qualitatively. One representative example is amphiphile-induced ordering transitions at LC/aqueous interfaces.

View Article Online
DOI: 10.1039/D6LF00103C

At low surface coverage, amphiphiles typically impose planar alignment, whereas at higher surface densities—typically above ~0.4–0.9 nm² per molecule—they induce homeotropic orientation.[10,44,45] This density threshold reflects the packing requirement for the alkyl chains to dominate the interfacial free energy landscape. The concentration difference required to cross this interfacial packing threshold directly matches the concentration window over which the LC sensor exhibits its highest optical contrast, meaning LOD is fundamentally determined by the interfacial density required to trigger an anchoring transition. In systems where probe amphiphiles and analytes bind in a 1:1 stoichiometry, the detectable analyte concentration is therefore predictable from the perturbation needed to shift the interface across the alignment boundary. [41,42]

Similarly, variations in alkyl chain length, head-group charge, or hydrogen-bonding capacity alter surface anchoring strength, which in turn sets the director tilt angle (θ) and ultimately the measured optical intensity or phase retardation. This relationship is not empirical, but it is governed by the elastic–anchoring balance discussed in Section 2.4, meaning that LC performance metrics can be mapped onto interfacial free-energy coordinates. These examples demonstrate that LC sensing behavior is not governed by "material sensitivity," but by where the system sits on the interface–alignment energy landscape (Fig. 3). Fig. 3D formalizes this concept by presenting a two-dimensional design map in which interfacial control parameters (e.g., amphiphilic packing density, anchoring free energy, elastic energy, and deviation in amphiphilicity) are plotted against LC alignment states (θ), with contours representing performance outputs such as LOD.

Establishing robust structure–property–performance relationships requires the integration of complementary characterization techniques capable of probing both the interface and the resulting LC response. Surface-sensitive methods such as XPS, FTIR, Raman spectroscopy, and AFM provide quantitative information regarding interfacial composition, chemical state,

View Article Online
DOI: 10.1039/D6LF00103C

molecular organization, and surface morphology. These measurements can be correlated with optical and electro-optical analyses that quantify LC alignment transitions, director-field reorganization, and signal transduction behavior. In this workflow, interfacial descriptors such as surface composition, charge density, binding affinity, roughness, and anchoring strength are linked to LC descriptors such as tilt angle, birefringence intensity, defect density, and response kinetics. These LC descriptors can then be mapped onto analytical sensing metrics, including sensitivity, selectivity, response time, detection limit, reversibility, and operational stability. Such quantitative correlations establish a rational framework for predictive sensor design, moving the field beyond empirical optimization toward interface-guided engineering of next-generation LC sensing platforms.

4.3 Sources of Non-Ideal Behavior: Defect-Mediated Signals and Interfacial Hysteresis

While LC sensors are often presented as binary systems with clean planar–homeotropic transitions, real interfaces seldom behave ideally. Two dominant sources of performance degradation are:

1. **Defect-mediated optical artifacts**

   A critical yet often overlooked limitation in LC sensing is the contribution of defect-driven optical artifacts. Topological structures such as boojums, disclinations, and Saturn-ring defects can generate bright or dark regions entirely independent of analyte binding, meaning that the optical output is not always a direct reporter of interfacial chemistry. These defects originate from nanoscale heterogeneity in surface energy, roughness, or clustered amphiphile domains, yet are frequently misinterpreted as "partial alignment transitions".[46] The result is a deceptive calibration landscape in which optical intensity no longer scales monotonically with concentration, giving rise to false-positive slopes, apparent signal plateaus, or non-linear dose–response

View Article Online
DOI: 10.1039/D6LF00103C

behavior.[47] Until the field distinguishes true chemical responses from defect-mediated artifacts, sensitivity metrics alone will remain insufficient to evaluate sensing reliability.

2. **Interfacial hysteresis and kinetic trapping**

   A second and equally consequential issue is interfacial hysteresis—an energetic bottleneck that emerges not from the LC bulk, but from the interfacial energy landscape itself. When anchoring energy changes are of the same order as elastic penalties, the LC can be trapped in metastable orientational states, producing slow, history-dependent, or incomplete switching cycles. This behavior is frequently mistaken for "poor LC reversibility," when in fact it reflects delayed interfacial relaxation caused by amphiphile rearrangement or incomplete desorption.[48] The recurring failure of many "high-sensitivity" LC sensors to reset across repeated cycles illustrates the same principle: the true rate-limiting step is not LC reorientation, but interfacial recovery. Recognizing this distinction is essential if LC sensors are to transition from single-use demonstrations to robust, operational devices.

These non-idealities underscore the central argument of this section: performance deviations in LC sensing are almost always interfacial in origin, even when they appear as optical artifacts. Eliminating these behaviors therefore requires not only optimizing the LC material but also engineering the interface.

4.4 Toward Predictive LC Sensor Design: Theory, Simulation, and Data-Driven Mapping

If the interface–alignment–performance relationship can be quantified, LC sensing can move from empirical tuning to first-principles prediction. Several emerging approaches listed in Table 2 make this feasible. Already, single-molecule simulations have accurately predicted the chain length thresholds required for homeotropic ordering, matching experimental values within ±0.2 nm² per molecule.[49] Likewise, machine-learning classifiers trained on POM

View Article Online
DOI: 10.1039/D6LF00103C

datasets can now distinguish defect-driven signals from true anchoring transitions with >95% accuracy, enabling automated rejection of false positives.[50] Taken together, these advances point toward a predictive LC sensing workflow:

Interface design (chemical / structural) → simulated LC alignment → predicted performance window → experimental validation

Rather than "test and observe," the field can shift to "design → simulate → fabricate", following the broader trajectory already seen in data-driven materials design, photonic sensing, and MOF-based sensing platforms.[51,52] This predictive workflow further requires a multiscale theory–experiment framework capable of linking molecular interfacial events, LC alignment responses, and device-level sensing metrics, as further discussed in Section 5.2.

Table 2. Hierarchical modeling strategies linking interfacial energetics to LC alignment states and macroscopic sensing performance.

Level	Method	Predictive Target	Ref.
Molecular	DFT, molecular dynamics	binding energy, anchoring strength, amphiphile orientation.	49, 50
Interfacial	coarse-grained & lattice models	packing density vs. tilt transition, defect nucleation.	26
Mesoscopic	Landau–de Gennes, finite-element LC elasticity	defect topology, optical output, hysteresis loop shape.	23
Data-driven	Machine learning image analysis & inverse design	concentration prediction, tilt reconstruction, optimal interface selection.	40, 41

5. Outlook: toward rational interfacial engineering for next-generation LC sensors

LC-based sensors are rapidly evolving from visually readable proof-of-concept platforms into sophisticated interfacial transducers capable of real-time chemical and biological monitoring. The preceding sections have shown that sensing performance in LC systems is governed not by bulk material properties, but by the chemistry, mechanics, and dynamics of

View Article Online
DOI: 10.1039/D6LF00103C

the interface. Accordingly, the future of LC sensing will depend on the transition from empirical tuning toward predictive, interface-guided design. Three converging research directions are expected to define this transition:

5.1 Programmable Interfacial Chemistry

The next generation of LC sensors will require interfaces that are not merely functionalized, but dynamically reconfigurable, responding selectively to molecular cues, pH shifts, ionic strength, light, temperature, or redox state. Such programmable interfaces would enable reversible tuning of anchoring energy, defect structure, and director geometry, allowing LC alignment to be modulated on demand rather than passively perturbed by analytes. Advances in supramolecular chemistry, dynamic covalent coatings, stimuli-responsive SAMs, and polymer-grafted interfaces are expected to enable self-regulating LC surfaces capable of amplification, reset, or adaptive thresholds.

5.2 Multiscale Modeling Coupled with Experiment

Interfacial events in LC sensors operate across coupled molecular (Å–nm), interfacial (nm–μm), and elastic (μm–mm) length scales. Progress will require integrated theory–experiment pipelines in which molecular dynamics, density functional theory (DFT) calculations, coarse-grained simulations, and continuum elastic models are validated against spectroscopic, optical, and topological imaging of LC alignment. At the molecular level, simulations can provide descriptors such as binding energy, adsorption geometry, molecular orientation, and analyte-induced changes in interfacial organization. At the interfacial and mesoscale levels, these descriptors can be translated into anchoring strength, director-field reorganization, defect nucleation, and response kinetics. When coupled with machine-learning-assisted texture analysis and data-driven optimization, this multiscale framework can establish quantitative structure–interface–response relationships, reduce reliance on trial-and-error

View Article Online
DOI: 10.1039/D6LF00103C

functionalization, and accelerate the rational development of high-performance, application-specific LC sensing platforms.

5.3 Data-Driven Interface–Performance Mapping

Because LC sensors inherently produce digitizable optical textures, they are uniquely suited for machine-learning-assisted sensing. AI-based analysis of texture evolution, defect topology, and grayscale dynamics offers a path toward establishing structure–interface–performance correlations that are not observable by human inspection. Data-driven platforms could (i) classify analytes from optical patterns, (ii) predict limit-of-detection based on interfacial parameters, and (iii) guide autonomous optimization of LC formulations and surface chemistries—accelerating discovery and enabling reproducible, scalable sensor engineering.

5.4 Remaining Barriers and Practical Requirements

Despite rapid advancements, several fundamental obstacles still limit the full deployment of LC-based sensors. Interfacial stability remains vulnerable in complex environments where competing amphiphiles, fluctuating ionic strength, or biofouling can disrupt anchoring conditions. In flexible or large-area devices, long-term operation often leads to the gradual accumulation of alignment defects, compromising signal uniformity. Equally critical is the persistent difficulty of decoupling true analyte-induced responses from background perturbations, which continues to constrain quantitative accuracy. Overcoming these barriers will require chemically robust anchoring layers, defect-tolerant alignment strategies, and AI-assisted signal correction capable of maintaining reliable performance outside controlled laboratory settings. Future advances are likely to emerge from nanopatterned interfaces, dynamic self-assembled monolayers, stimuli-responsive surface coatings, and operando characterization techniques that provide precise control and real-time insight into interfacial evolution during sensing.

View Article Online
DOI: 10.1039/D6LF00103C

5.5 Toward Interface-Guided Design of LC Sensors

The trajectory of the field is clear: LC sensing will mature only when interfacial phenomena can be engineered with the same precision that optical or electro-optical properties are measured. Real progress will require interdisciplinary convergence across surface chemistry, soft matter physics, optical engineering, and data science. As LC sensors evolve from observational platforms to rationally programmed interfacial systems, they will enable predictive, programmable, and multifunctional detection technologies suitable for environmental monitoring, biomedical diagnostics, and adaptive intelligent materials. In short, the future of LC sensing may rely not only on developing improved LC materials and their corresponding sensing mechanism, but also on advancing interfacial design together with the capability to visualize and algorithmically control interfacial behavior. Meaningful progress is likely to emerge when LC sensors are understood and developed through interfacial principles rather than interpreted solely from optical textures.

Author Information

Corresponding Author

Chih-Hsin Chen - *Department of Chemistry, Tamkang University, New Taipei City 25137, Taiwan*

Email: chc@mail.tku.edu.tw

Authors

Rajib Nandi - *Department of Chemistry, Tamkang University, New Taipei City 25137, Taiwan*

Muhammad Umer Saeed - *Department of Chemistry, Tamkang University, New Taipei City 25137, Taiwan*

Author contributions

View Article Online
DOI: 10.1039/D6LF00103C

Rajib Nandi: Conceptualization, literature survey, data curation, visualization, and original draft preparation. Muhammad Umer Saeed: Literature survey, visualization, and manuscript revision. Chih-Hsin Chen: Conceptualization, supervision, funding acquisition, project administration, and writing – review and editing.

Conflicts of interest

There is no conflict of interest to declare.

Acknowledgements

The authors gratefully acknowledge financial support from the National Science and Technology Council, Taiwan (Grant Numbers. NSTC 113-2113-M-032-002, 114-2113-M-032-002, 113-2811-M-032-004, and 114-2811-M-032-007).

References

1. R. Nandi, M. U. Saeed and C.-H. Chen, *Sens. Actuators, B*, 2025, **446**, 138684, DOI: 10.1016/j.snb.2025.138684.
2. Y. Choi, D. Choi, J.-K. Choi, K.-S. Oh, E. Cho, J.-H. Im, D. P. Singh and Y.-K. Kim, *ACS Appl. Opt. Mater.*, 2023, **1**, 1879–1897, DOI: 10.1021/acsaom.3c00282.
3. Z. Rouhbakhsh, J.-W. Huang, T. Y. Ho and C.-H. Chen, *TrAC, Trends Anal. Chem.*, 2022, **157**, 116820, DOI: 10.1016/j.trac.2022.116820.
4. D. Wang, S.-Y. Park and I.-K. Kang, *J. Mater. Chem. C*, 2015, **3**, 9038–9047, DOI: 10.1039/C5TC01321F.
5. R. J. Carlton, J. T. Hunter, D. S. Miller, R. Abbasi, P. C. Mushenheim, L. N. Tan and N. L. Abbott, *Liq. Cryst. Rev.*, 2013, **1**, 29–51, DOI: 10.1080/21680396.2013.769310.
6. C. Esteves, E. Ramou, A. R. P. Porteira, A. J. Moura Barbosa and A. C. A. Roque, *Adv. Opt. Mater.*, 2020, **8**, 1902117, DOI: 10.1002/adom.201902117.
7. J. M. Brake, M. K. Daschner, Y. Y. Luk and N. L. Abbott, *Science*, 2003, **302**, 2094–2097, DOI: 10.1126/science.1091749.
8. I. Pani, S. Sil and S. K. Pal, *Langmuir*, 2023, **39**, 909–917, DOI: 10.1021/acs.langmuir.2c02959.
9. R. Nandi, V. Jain, T. Gupta and S. K. Pal, *Colloids Surf., A*, 2021, **625**, 126952, DOI: 10.1016/j.colsurfa.2021.126952.

10. I.-H. Lin, D. S. Miller, P. J. Bertics, C. J. Murphy, J. J. de Pablo and N. L. Abbott, *Science*, 2011, **332**, 1297–1300, DOI: 10.1126/science.1195639.

11. H. Yu, J. I. Gold, T. J. Wolter, N. Bao, E. Smith, H. A. Zhang, R. J. Twieg, M. Mavrikakis and N. L. Abbott, *Adv. Mater.*, 2024, **36**, 2309605, DOI: 10.1002/adma.202309605.

12. R. Nandi, Y.-Y. Yeh, P.-S. Pan and C.-H. Chen, *Microchem. J.*, 2026, **221**, 117067, DOI: 10.1016/j.microc.2026.117067.

13. Y.-K. Kim, X. Wang, P. Mondkar, E. Bukusoglu and N. L. Abbott, *Nature*, 2018, **557**, 539–544, DOI: 10.1038/s41586-018-0098-y.

14. F. Xu, Y. Yang, X. Feng and X. Lu, *Nat. Commun.*, 2026, **17**, 1367, DOI: 10.1038/s41467-025-68116-2.

15. A. Chatterjee, A. Joy and P. Purkayastha, *Langmuir*, 2024, **40**, 4321–4332, DOI: 10.1021/acs.langmuir.3c03588.

16. Leal-Junior, M. S. Soares, P. M. de Almeida and C. Marques, *Adv. Sensor Res.*, 2023, **2**, 2300022, DOI: 10.1002/adsr.202300022.

17. P.-H. Chiang, B. P. Singh and S.-J. Hwang, *Sens. Actuators, A*, 2026, **399**, 117461, DOI: 10.1016/j.sna.2026.117461.

18. S. Aery, A. Parry, A. Araiza-Calahorra, S. D. Evans, H. F. Gleeson, A. Dan and A. Sarkar, *J. Mater. Chem. C*, 2023, **11**, 5831–5845, DOI: 10.1039/d3tc00598d.

19. T. Gupta, A. P. Menon, S. Kapoor and S. K. Pal, *J. Mater. Chem. B*, 2025, **13**, 8059–8067, DOI: 10.1039/D4TB02602K.

20. M. A. Bedolla Pantoja, Y. Yang and N. L. Abbott, *Liq. Cryst.*, 2019, **46**, 1925–1936, DOI: 10.1080/02678292.2019.1633432.

21. Y.-J. Chuang, R. Nandi and C.-H. Chen, *Anal. Chim. Acta*, 2025, **1338**, 343582, DOI: 10.1016/j.aca.2024.343582.

22. D. S. Miller, R. J. Carlton, P. C. Mushenheim and N. L. Abbott, *Langmuir*, 2013, **29**, 3154–3169, DOI: 10.1021/la304679f.

23. P. G. de Gennes and J. Prost, *The Physics of Liquid Crystals*, 2nd edn, Oxford University Press, Oxford, 1993.

24. P. Poulin, H. Stark, T. C. Lubensky and D. A. Weitz, *Science*, 1997, **275**, 1770–1773, DOI: 10.1126/science.275.5307.1770.

25. I. Muševič, M. Škarabot, U. Tkalec, M. Ravnik and S. Žumer, *Science*, 2006, **313**, 954–958, DOI: 10.1126/science.1129660.

26. N. A. Lockwood, J. K. Gupta and N. L. Abbott, *Surf. Sci. Rep.*, 2008, **63**, 255–293, DOI: 10.1016/j.surfrep.2008.02.002.

27. M. Škarabot and I. Muševič, *Soft Matter*, 2010, **6**, 5476–5481, DOI: 10.1039/B807979J.

28. X. Wang, D. S. Miller, E. Bukusoglu, J. J. de Pablo and N. L. Abbott, *Nat. Mater.*, 2016, **15**, 106–112, DOI: 10.1038/nmat4421.

29. I. I. Smalyukh, Y. Lansac, N. A. Clark and R. P. Trivedi, *Science*, 2011, **334**, 79–83, DOI: 10.1126/science.1209997.

30. I. Verma, M. Devi, D. Sharma, R. Nandi and S. K. Pal, *Langmuir*, 2019**,** *35*, 7816–7823. DOI: 10.1021/acs.langmuir.8b04018.

31. X. Wang, P. Yang, F. Mondiot, Y. Li, D. S. Miller, Z. Chen and N. L. Abbott, *Chem. Commun.*, 2015, **51**, 9576–9579, DOI: 10.1039/C5CC06996C.

32. M. S. Ibrahim, M.-S. Lee, S. Park, A. Naman, D. Lee, Y. Kwak and M. Kim, *TrAC, Trends Anal. Chem.*, 2025, **193**, 118426, DOI: 10.1016/j.trac.2025.118426.

33. G. Barnes and I. Gentle, Interfacial Science: An Introduction, 2nd edn, Oxford University Press, Oxford, 2011.

34. G. L. Richmond, *Chem. Rev*., 2002, **102**, 2693–2724. DOI: 10.1021/cr0006876.

35. X. Wang, X. Gao, H. Zhong, K. Yang, B. Zhao, J. Deng, *Adv. Mater*. 2025, **37**, 2412805. https://doi.org/10.1002/adma.202412805.

36. S. Li, Z. Chen, P. Chen, Y. Wang, B. Wu, H. Tang, J. Zhao, J. Rho, L. Jiang and L. Chen, *Light Sci. Appl.*, 2024, 13, 27. https://doi.org/10.1038/s41377-023-01360-7.

37. M. Vera-Arévalo and A. Concellón, Fluorescence transduction of liquid crystal ordering transitions for biosensing, J. Am. Chem. Soc., 2026, 148, 3167–3173. DOI: 10.1021/jacs.5c16679.

38. I. Kim, W.-S. Kim, K. Kim, M. A. Ansari, M. Q. Mehmood, T. Badloe, Y. Kim, J. Gwak, H. Lee, Y.-K. Kim and J. Rho, *Sci. Adv*., 2021, **7**, eabe9943. https://doi.org/10.1126/sciadv.abe9943.

39. M. A. Pimenta, G. C. Resende, H. B. Ribeiro and B. R. Carvalho, *Phys. Chem. Chem. Phys.*, 2021, **23**, 27103–27123, DOI: 10.1039/D1CP03626B.

40. Y. Cao, H. Yu, N. L. Abbott and V. M. Zavala, *ACS Sens.*, 2018, **3**, 2237–2245, DOI: 10.1021/acssensors.8b00100.

41. Y. Zhang, S. Xu, R. Zhang, Z. Deng, Y. Liu, J. Tian, Y. Lu, Q. Hu and Q. Ye, *Anal. Chem.*, 2022, **94**, 12781–12787, DOI: 10.1021/acs.analchem.2c02593.

42. S. K. Singh, R. Nandi, K. Mishra, H. K. Singh, R. K. Singh and B. Singh, *Sens. Actuators, B*, 2016, **226**, 381–387, DOI: 10.1016/j.snb.2015.11.077.

43. T. T. Ho, C. W. Hsu and C.-H. Chen, *Microchem. J.*, 2023, **188**, 108472, DOI: 10.1016/j.microc.2023.108472.

44. J. K. Gupta and N. L. Abbott, *Langmuir*, 2009, **25**, 2026–2033, DOI: 10.1021/la803475c.

45. X. Yang, X. Liang, R. Nandi, Y. Tian, Y. Zhang, Y. Li, J. Zhou, Y. Dong, D. Liu, Z Zhong and Z. Yang, *Biosensors*, 2022, **12**, 275, DOI: 10.3390/bios12050275.

46. P. Popov, E. K. Mann and A. Jákli, *Phys. Rev. Appl.*, 2014, **1**, 034003, DOI: 10.1103/PhysRevApplied.1.034003.

47. S. Maiti, M. Taghavi, P. Chaudhari, S. Roh, I. Cohen, A. B. Apsel and N. L. Abbott, *ACS Sens.*, 2025, **10**, 1870–1879, DOI: 10.1021/acssensors.4c02913.

48. H. Yu, T. Szilvási, K. Wang, J. I. Gold, N. Bao, R. J. Twieg, M. Mavrikakis and N. L. Abbott, *J. Am. Chem. Soc.*, 2019, **141**, 16003–16013, DOI: 10.1021/jacs.9b08057.

49. N. Bao, J. I. Gold, J. K. Sheavly, J. J. Schauer, V. M. Zavala, R. C. Van Lehn, M. Mavrikakis and N. L. Abbott, *J. Am. Chem. Soc.*, 2022, **144**, 16378–16388, DOI: 10.1021/jacs.2c03424.

50. J. I. Gold, J. K. Sheavly, N. Bao, H. Yu, J. Rajbangshi, J. J. Schauer, V. M. Zavala, N. L. Abbott, R. C. Van Lehn and M. Mavrikakis, *ACS Nano*, 2023, **17**, 22620–22631, DOI: 10.1021/acsnano.3c06735.

51. A. Ramola, A. K. Shakya, V. Kumar and A. Bergman, *Micromachines*, 2025, **16**, 747. https://doi.org/10.3390/mi16070747.

52. G. Benedetto, P. Damacet, E. O. Shehayeb, G. Fabusola, C. M. Simon and K. A. Mirica, *ACS Sens.*, 2025, **10**, 7787–7798. https://doi.org/10.1021/acssensors.5c02182.

View Article Online
DOI: 10.1039/D6LF00103C

Data availability statement

This Perspective article does not report any new data. No datasets were generated or analyzed during the current study.